Clemson University
College of Engineering and Science
Control and Robotics (CRB) Technical Report

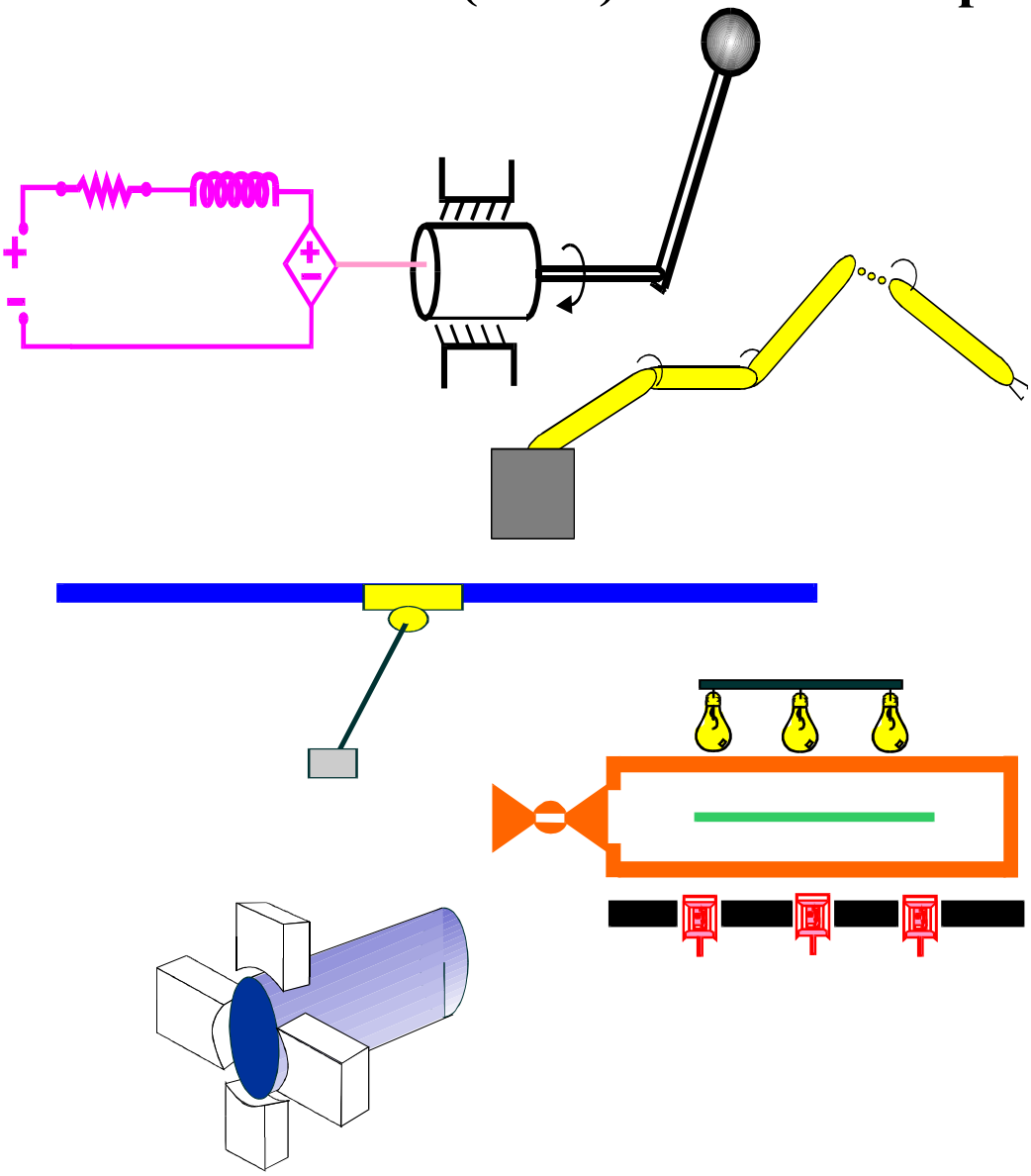

Number: CU/CRB/3/3/04/#1.pdf

Title: A Novel Passive Path Following Controller for a Rehabilitation Robot

Authors: X. Zhang, A. Behal, D.M. Dawson, and J. Chen

Report Documentation Page

Form Approved
OMB No. 0704-0188

1. REPORT DATE	2. REPORT TYPE	3. DATES COVERED
2004		**00-00-2004 to 00-00-2004**

4. TITLE AND SUBTITLE	5a. CONTRACT NUMBER
A Nove Passive Path Following Controller for a Rehabilitation Robot	5b. GRANT NUMBER
	5c. PROGRAM ELEMENT NUMBER
6. AUTHOR(S)	5d. PROJECT NUMBER
	5e. TASK NUMBER
	5f. WORK UNIT NUMBER
7. PERFORMING ORGANIZATION NAME(S) AND ADDRESS(ES) **Clemson University,Department of Electrical & Computer Engineering,Clemson,SC,29634-0915**	8. PERFORMING ORGANIZATION REPORT NUMBER
9. SPONSORING/MONITORING AGENCY NAME(S) AND ADDRESS(ES)	10. SPONSOR/MONITOR'S ACRONYM(S)
	11. SPONSOR/MONITOR'S REPORT NUMBER(S)

12. DISTRIBUTION/AVAILABILITY STATEMENT
Approved for public release; distribution unlimited

13. SUPPLEMENTARY NOTES
The original document contains color images.

14. ABSTRACT

15. SUBJECT TERMS

16. SECURITY CLASSIFICATION OF:			17. LIMITATION OF ABSTRACT	18. NUMBER OF PAGES	19a. NAME OF RESPONSIBLE PERSON
a. REPORT	b. ABSTRACT	c. THIS PAGE			
unclassified	**unclassified**	**unclassified**		**12**	

A Novel Passive Path Following Controller for a Rehabilitation Robot[1]

X. Zhang[‡], A. Behal[†], D.M. Dawson[‡], and J. Chen[‡]

[†]Department of Electrical and Computer Engineering, Clarkson University, Potsdam, NY 13699-5720

[‡]Department of Electrical and Computer Engineering, Clemson University, Clemson, SC 29634-0915

E-mail: abehal@clarkson.edu; xzhang,ddawson,jianc@clemson.edu

Abstract

In this paper, we present a path generation and control strategy for a robotic manipulator to mimic the dynamics of a continuously reconfigurable anisotropic impedance. Motivated by a nonholonomic kinematic constraint, a dynamic path generator is designed to trace a desired contour in the robot's workspace when an interaction force is applied at the robot's end-effector. The proposed continuous control strategy achieves semi-global asymptotically stable path following for the robot manipulator in the presence of uncertainty in the robot dynamics. Additionally, the path generator also ensures safety by maintaining the desired net flow of energy during the human robot interaction from the user toward the manipulator. In addition to providing asymptotic path following, the control algorithm also ensures sufficiently rapid error convergence at the end-effector such that the actual energy transfer profile follows the desired energy transfer profile - thus rigorously ensuring user safety. A variation of the generation and control algorithms is presented to deal with unknown interaction force at the end-effector.

1 Introduction

Typically, robots are used for simple, repetitive tasks in structured environments isolated from humans. However, the last decade has seen a surge in active research in the area of human robot interaction. Bilateral teleoperated robots [4, 9, 10, 22], smart exercise machines [11, 12], human assist gantry cranes [20], rehabilitation robots [3, 8, 13, 14], and steer-by-wire applications [16, 17] are among the multitude of application areas that drive this research. A common objective of the control algorithm design in all human robot interface applications is to rigorously ensure user safety. Approaches based on passivity ensure that the net flow of energy during the human robot interaction is from the user to the machine [1, 11].

The problem that is dealt with in this paper attempts to cast the robot as a reconfigurable passive exercise machine and is inspired by the desire to provide passive resistance therapy to patients affected by dystrophies in the muscles of the upper extremities that must target specific groups of muscles in order to regain muscle tone [2]. Along any desired curve of motion in 3D space that satisfies a criterion of merit, motion is permitted against a programmable apparent inertia when the user "pushes" at the end-effector; force applied in all other directions is penalized. In the simplest sense, the robot essentially acts like a "wheel" (with programmable inertial feel for the user) on an arbitrary smooth contoured rail that is driven by the user force at the robot end-effector. In order to address concerns of the robot running out of its workspace and into singularities, we allow for an optional spring attached to the "wheel" that winds up and down as the "wheel" rotates and provides for workspace dependent resistance; this ensures that a bounded interaction force leads to bounded desired trajectories.

The strategy proposed in this paper achieves semi-global asymptotically stable path following for an $n-$link revolute robot manipulator in the presence of uncertainty in the robot dynamics. Specifically, given a desired curve of motion that optimizes apriori established merit criteria, we design a generator based on an anisotropic force-velocity relationship that generates a bounded desired trajectory in the robot workspace given the interaction force at the end-effector as well as generator parameters as the inputs into the generator. The reference trajectory generator is carefully designed in order to ensure that the relationship between the interaction force and the desired end-effector velocity satisfies a passivity constraint. Next, a control strategy is crafted using a Lyapunov based argument in order to obtain the companion objectives of driving the end-effector tracking error to zero and ensuring that a filtered error signal satisfies an $\mathcal{L}_1$ property. This convergence of the filtered error signal allows us to ensure that the interaction of the user with the robot is passive, *i.e.*, energy always flows from the user to the robot

[1]This work is supported in part by two DOC Grants, an ARO Automotive Center Grant, a DOE Contract, a Honda Corporation Grant, and a DARPA Contract.

manipulator. Additionally, a readily satisfiable mild assumption on the differentiability of the robot dynamics allows us to generate a control strategy that is continuous; this has significant implications in terms of implementability of the control algorithm. As an aside, the control mechanism has the interesting feature of being able learn the unknown robot dynamics dynamics. We also present an extension of our controller to the case when the interaction force measurement at the end-effector is either unreliable or unmeasurable. In this case, we are able to demonstrate global asymptotically stable path following when the robot dynamics are known.

This paper is organized as follows. Section 2 of the paper presents details of the path generation algorithm. In Section 3, we transform the robot dynamics into a non-inertial frame amenable to our control design. In Section 4, we define the error systems, measurement constraints, and the assumptions under which the analysis is valid. In Section 5, we present the design of the control strategy. Section 6 analyzes the stability of the closed-loop systems in addition to demonstrating the accomplishment of control objectives laid out in Section 4. In Section 7, we present an extension of the control algorithm to the case of unmeasurable interaction force. Simulation results are presented in Section 8.

2 Path Planning

In this section, we set up a reference generator to obtain a desired trajectory for the motion of the robot end-effector in 3D Cartesian space. Consider an operator specified[1] desired curve of motion $\bar{r}_d(s) \in \Re^3$ given as follows

$$\bar{r}_d(s) = x_d(s)\,\hat{\imath} + y_d(s)\,\hat{\jmath} + z_d(s)\,\hat{k} \tag{1}$$

where $s(t) \in \Re^1$ is an arbitrary parameter along the curve, while $x_d(s)$, $y_d(s)$, and $z_d(s) \in \Re^1$ represent the respective coordinates in an inertial frame $\mathcal{I}$ (say fixed to the base of the robot). Let $v_{dc}(t) \in \Re^1$ be the yet to be chosen speed along the curve; one can then define the following expression for $\dot{s}(t) \in \Re^1$ as follows

$$\dot{s} = v_{dc}\left(\bar{r}_d'(s) \cdot \bar{r}_d'(s)\right)^{-1/2} \tag{2}$$

Let $\mathcal{F} = \left(\bar{u}(s), \bar{p}(s), \bar{b}(s)\right)$ be a rotating frame[2] associated with the curve $\bar{r}_d(s)$ such that

$$\begin{aligned} \bar{u}(s) &= \frac{\bar{r}_d'(s)}{|\bar{r}_d'(s)|} \qquad & \bar{p}(s) &= \frac{\bar{u}'(s)}{|\bar{u}'(s)|} \\ \bar{b}(s) &= \bar{u}(s) \times \bar{p}(s) \end{aligned} \tag{3}$$

[1] For a rehabilitation application, $\bar{r}_d(s)$ would be chosen by a physical therepist in order for a target set of muscles to be exercised during a particular therapy session, *e.g.*, maximizing range of motion or power output for a target muscle set.

[2] The origin of the frame $\mathcal{F}$ is chosen to coincide with the inertial frame $\mathcal{I}$.

We also define the curvature $\kappa(s)$ and torsion $\tau(s)$ associated with the curve as follows

$$\begin{aligned} \kappa(s) &= |\bar{u}'(s)| \\ \tau(s) &= -\bar{p}(s) \cdot \bar{b}'(s) \end{aligned} \tag{4}$$

We next define $x_d(s,t) \in \Re^3$ to be the desired position of the robot end-effector expressed in the following manner

$$x_d = \gamma_{d1}\bar{u} + \gamma_{d2}\bar{p} + \gamma_{d3}\bar{b} = \Gamma(s)\,\gamma_d \tag{5}$$

where $\Gamma(s) = \begin{bmatrix} \bar{u}(s) & \bar{p}(s) & \bar{b}(s) \end{bmatrix} \in SO(3)$ is obviously defined and $\gamma_d(t) = \begin{bmatrix} \gamma_{d1}(t) & \gamma_{d2}(t) & \gamma_{d3}(t) \end{bmatrix}^T \in \Re^3$ denotes desired end-effector position coordinates in $\mathcal{F}$. By time differentiating (5) and utilizing (3) and (4), one can obtain the following relationship

$$\dot{\gamma}_d = \dot{s}\,[u]_\times\,\gamma_d + v_d \qquad \gamma_d(0) = \Gamma^T(s(t_0))\,x_{d0} \tag{6}$$

where $[u(s)]_\times \in \Re^{3\times 3}$ is the antisymmetric matrix associated with the vector $u(s) = \begin{bmatrix} -\tau(s) & 0 & -\kappa(s) \end{bmatrix}^T \in \Re^3$, $v_d(t) = \begin{bmatrix} v_{d1}(t) & v_{d2}(t) & v_{d3}(t) \end{bmatrix}^T \in \Re^3$ denotes desired end-effector velocity coordinates in $\mathcal{F}$, $x_{d0} \in \Re^3$ denotes a suitably chosen point in the interior of the robot's workspace, while t_0 denotes initial time. In order to impose the constraint that the desired robot end-effector trajectory $x_d(\cdot)$ does not move in the direction of the normal and the binormal to $\bar{r}_d(s)$, we must ensure the following nonholonomic kinematic constraint

$$v_{d2} = v_{d3} = 0 \tag{7}$$

In order to enforce this kinematic constraint, we implement an asymmetric impedance relationship between the user applied force and the desired end-effector velocity as follows

$$M_\Gamma \dot{v}_d + B_\Gamma v_d + k_\Gamma \tilde{\gamma}_d = F_f \tag{8}$$

where $M_\Gamma = diag\{m_1, m_2, m_3\}$ denotes a positive-definite desired inertia matrix, $B_\Gamma = diag\{b_1, b_2, b_3\}$ denotes a positive-definite desired damping matrix, $k_\Gamma \in \Re^1$ denotes a non-negative stiffness constant, $F_f(t) = \begin{bmatrix} f_u(t) & f_p(t) & f_b(t) \end{bmatrix}^T \in \Re^3$ denotes the user applied force expressed in $\mathcal{F}$, while $\tilde{\gamma}_d(t) \in \Re^3$ denotes an error signal that is defined as follows

$$\tilde{\gamma}_d = \gamma_d - \Gamma^T(s(t))\,\Gamma(s(t_0))\,\gamma_d(t_0). \tag{9}$$

One can now designate arbitrary damping b_1 along the tangent as well as arbitrarily large damping b_2 and b_3 along the normal and the binormal in order to enforce (7). With this choice of the desired damping matrix, the desired speed of the robot end-effector along the curve is $v_{d1}(t)$. Motivated by the dynamics of (8) and the desire to ensure that the motion along the desired curve $\bar{r}_d(s)$ corresponds to the user application of force

at the end-effector, we choose $v_{dc}(t) = v_{d1}(t)$ such that $s(t)$ evolves according to the following dynamics

$$\dot{s} = v_{d1}\left(\bar{r}_d'(s) \cdot \bar{r}_d'(s)\right)^{-1/2} \tag{10}$$

where (2) has been utilized. We note here the special case when s is the arc length parameter, then $\bar{r}'(s) \cdot \bar{r}'(s) = 1$ and consequentially $\dot{s} = v_{d1}$ is the speed along the curve.

In order for a user to exercise safely in conjunction with the robot, the robot must act as a passive device, i.e., the work done by the user force is always positive (minus finite stored initial energy if any). With that objective in mind, we first demonstrate that

$$\int_{t_0}^{t} \bar{F}_f \cdot \bar{v}_d dt \geq -c^2 \Rightarrow \int_{t_0}^{t} v_d^T F_f dt \geq -c_1^2 \tag{11}$$

where $\bar{F}_f(t), \bar{v}(t) \in \Re^3$ denote the user force and desired end-effector velocity vectors, respectively, while c_1^2 is a bounded, positive scalar. In order to prove (11), we define a Lyapunov function

$$V = \frac{1}{2} v_d^T M_\Gamma v_d + \frac{1}{2} k_\Gamma \tilde{\gamma}_d^T \tilde{\gamma}_d \geq 0 \tag{12}$$

After taking the time derivative of (12) along the desired dynamics of (6) and (8), we obtain

$$\dot{V} = -v_d^T B_\Gamma v_d + v_d^T F_f \tag{13}$$

where we have utilized the definition of (9) and the fact that $[u(s)]_\times$ is antisymmetric. After rearranging terms in the above equation and integrating both sides, one can obtain

$$\int_{t_0}^{t} v_d^T F_f dt = V(t) - V(t_0) + \int_{t_0}^{t} v_d^T B_\Gamma v_d dt \tag{14}$$

After utilizing the fact that $V(t), v_d^T B_T v_d \geq 0$, we can obtain an lowerbound for the left hand side of the above equation as follows

$$\int_{t_0}^{t} v_d^T F_f dt \geq -V(t_0) = -c_1^2 \tag{15}$$

which proves (11). In the sequel, we will show passivity of the robot by utilizing (15) and the yet to be proved $\mathcal{L}_1$ stability of the end-effector velocity tracking error.

Remark 1 *If k_Γ of (8) is chosen to be zero, it is possible that the desired trajectory $\gamma_d(t)$ might lie outside the robot's finite workspace. In that case, one may constrain $\gamma_d(t)$ to lie inside the robot workspace via a proper selection of initial conditions and the desired curve $\bar{r}_d(s)$. If the desired robot is chosen to have non-zero stiffness, the reference generator dynamics described above constrain the desired robot to mimic the motion of a wheel on a contoured rail tethered to a spring that is unstretched when the desired robot end-effector is at x_{d0}; this spring winds and unwinds as the wheel rotates. A properly chosen interior point x_{d0} and stiffness k_Γ ensure that a bounded interaction force leads to desired trajectories that always lie inside the robot's workspace.*

3 Robot Dynamics

The dynamic model for an n-link, revolute direct drive robot manipulator is assumed to be in the following form [19]

$$M(q)\ddot{q} + V_m(q,\dot{q})\dot{q} + G(q) = \tau_q + F_q \tag{16}$$

where $M(q) \in \Re^{n\times n}$ represents the inertia matrix, $V_m(q,\dot{q}) \in \Re^{n\times n}$ represents the centripetal-Coriolis matrix, $G(q) \in \Re^n$ represents the gravity effects, $F_q \in \Re^n$ represents the user applied force expressed in joint space, and $\tau_q(t) \in \Re^n$ represents the torque input vector.

The end-effector position in the inertial frame $\mathcal{I}$, denoted by $x(t) \in \Re^3$, is defined as follows

$$x = f(q) \tag{17}$$

where $f(q) \in \Re^3$ denotes the robot forward kinematics, and $q(t) \in \Re^n$ denotes the link position. Based on (17), the differential relationships between the end-effector position and the link position variables can be calculated as follows

$$\begin{aligned} \dot{x} &= J(q)\,\dot{q} \\ \ddot{x} &= \dot{J}(q)\dot{q} + J(q)\ddot{q} \end{aligned} \tag{18}$$

where $\dot{q}(t), \ddot{q}(t) \in \Re^n$ denote the link velocity and acceleration vectors, respectively, and $J(q) = \dfrac{\partial f(q)}{\partial q} \in \Re^{3\times n}$ denotes the manipulator Jacobian. After utilizing (17) and (18), one can transform the joint space dynamics into the task-space as follows

$$\bar{M}(x)\ddot{x} + \bar{V}_m(x,\dot{x})\dot{x} + \bar{G}(x) = \tau_x + F_x \tag{19}$$

where $\bar{M}(\cdot) = J^{+T} M J^+, \bar{V}_m(x,\dot{x}) = -J^{+T} M J^+ \dot{J} J^+ + J^{+T} V_m J^+ \in \Re^{3\times 3}$ denote, respectively, transformed inertia and centripetal-Coriolis matrices, $\bar{G}(x) = J^{+T} G \in \Re^3$ represents gravity effects, $F_x(t) = J^{+T} F_q \in \Re^3$ represents the user applied force expressed in $\mathcal{I}$, $\tau_x(t) = J^{+T}\tau_q \in \Re^3$ represents the torque input vector expressed in $\mathcal{I}$, while $J^+(q) \in \Re^{n\times 3}$ denotes a pseudo-inverse of the manipulator Jacobian $J(q)$. The relationship between the end-effector position expressed in the coordinates of $\mathcal{I}$ and $\mathcal{F}$ can be expressed as

$$x = \Gamma(s)\,\gamma \tag{20}$$

where $\Gamma(s), x(t)$ have been previously defined and we define $\gamma(t)$ to be the robot end-effector position coordinates in $\mathcal{F}$. After utilizing the above relationship, one

can obtain the robot dynamics in $\mathcal{F}$ as follows

$$M_f(\gamma)\ddot{\gamma} + V_f(\gamma,\dot{\gamma})\dot{\gamma} + G_f(\gamma) = \tau_f + F_f \tag{21}$$

where $M_f(\cdot), V_f(\cdot) \in \Re^{3\times 3}$ denote, respectively, transformed inertia and centripetal-Coriolis matrices, $G_f(\cdot) \in \Re^3$ represents gravity effects, $F_f(t) = \Gamma^T F_x \in \Re^3$ represents the user applied force expressed in $\mathcal{F}$, while $\tau_f(t) = \Gamma^T \tau_x \in \Re^3$ represents the torque input vector expressed in $\mathcal{F}$. Motivated by the subsequent stability analysis and control design, we state the following property:

Property 1: The inertia matrix $M_f(\cdot)$ is symmetric and positive-definite, and satisfies the following inequalities

$$\underline{m}\,\|\xi\|^2 \leqslant \xi^T M_f(\cdot)\,\xi \leqslant \overline{m}(\gamma)\,\|\xi\|^2 \qquad \forall \xi \in \Re^3 \tag{22}$$

where $\underline{m} \in \Re$ denotes a positive constant, $\overline{m}(\gamma) \in \Re$ denotes a positive nondecreasing function, while $\|\cdot\|$ denotes the standard Euclidean norm.

4 Problem Formulation

Given the desired robot end-effector trajectory $\gamma_d(t)$ (obtained via on-line solution of (6), (8), and (10)), our primary control objective is to asymptotically drive the end-effector trajectory tracking error

$$e_1 \triangleq \gamma_d - \gamma \tag{23}$$

to zero while compensating for uncertainties in the system dynamics. Motivated by the subsequent control design strategy, we introduce additional tracking error variables $e_2(t), r(t) \in \Re^3$ as follows

$$e_2 \triangleq \dot{e}_1 + e_1 \tag{24}$$

$$r \triangleq \dot{e}_2 + e_2 \tag{25}$$

Our secondary control objective is to preserve the passivity of the robot for safety of user operation in the sense that

$$\int_{t_0}^{t} v^T F_f dt \geq -c^2 \tag{26}$$

where $v(t)$ is the velocity of the robot and $F_f(t)$ is the interaction force. The control challenge is to obtain the companion objectives mentioned above while utilizing only measurements of the end-effector position, velocity, and the interaction force. Given these measurements, $e_1(t), e_2(t)$ are measurable variables while $r(t)$ is unmeasurable. Motivated by the ensuing control development and stability analysis, we make the following set of assumptions

Assumption 1 The transformed inertia, centripetal-Coriolis, and gravity matrices denoted, respectively, by $M_f(\cdot), C_f(\cdot)$, and $G_f(\cdot)$ are uncertain but known to be second order differentiable.

Assumption 2 $F_f(t) \in \mathcal{L}_\infty$ is a measurable interaction force at the end-effector.

Assumption 3 The reference trajectory $\gamma_d(t)$ is continuously differentiable up to its fourth derivative such that $\gamma_d^{(i)} \in \mathcal{L}_\infty, \quad i = 0,1,2,3,4.$

Assumption 4 The parameter s along the desired curve $\bar{r}_d(s)$ is continuously differentiable up to its third derivative such that $s^{(i)} \in \mathcal{L}_\infty, \quad i = 0,1,2,3.$

Assumption 5 The skew matrix $[u]_\times$ is continuously differentiable up to its second derivative such that $[u]_\times^{(i)} \in \mathcal{L}_\infty, \quad i = 0,1,2.$

Assumption 6 During the control development, we will make the assumption that the minimum singular value of the manipulator Jacobian, denoted by σ_m is greater than a known small positive constant $\delta > 0$, such that $\max\{\|J^+(q)\|\}$ is known a priori and all kinematic singularities are always avoided (Also see Remark 1). We also note that since we are only concerned with revolute robot manipulators, we know that kinematic and dynamic terms denoted by $M(q)$, $V_m(q,\dot{q})$, $G(q)$, $x(q)$, $J(q)$, and $J^+(q)$ are bounded for all possible $q(t)$ (*i.e.*, these kinematic and dynamic terms only depend on $q(t)$ as arguments of trigonometric functions). From the preceding considerations, it is easy to argue that $\bar{M}(x), \bar{C}(x,\dot{x}), \bar{G}(x), M_f(\gamma), V_f(\gamma,\dot{\gamma}), G_f(\gamma) \in \mathcal{L}_\infty$ for all possible $x(t), \dot{x}(t), \gamma(t), \dot{\gamma}(t)$.

5 Control Design

As a primary step, we partially feedback linearize the system by designing the control signal $\tau_f(t)$ as follows

$$\tau_f = -F_f + \bar{\tau}_f. \tag{27}$$

where $\bar{\tau}_f(t) \in \Re^3$ is a yet to be designed auxiliary control signal and we have taken advantage of Assumption 2. Additionally, we simplify the system representation of (21) by defining a generalized variable $B_f(\gamma,\dot{\gamma}) \in \Re^3$ as follows

$$B_f = V_f(\gamma,\dot{\gamma})\,\dot{\gamma} + G_f(\gamma). \tag{28}$$

The utilization of (27) and (28) allows us to succinctly rewrite (21) as follows

$$M_f\ddot{\gamma} + B_f = \bar{\tau}_f. \tag{29}$$

Given (23-25) and (29), we can obtain the open-loop tracking error dynamics as follows

$$M_f\dot{r} = -\frac{1}{2}\dot{M}_f r - e_2 - \dot{\bar{\tau}}_f + N \tag{30}$$

where $N(\cdot) \in \Re^3$ is an aggregation of unknown dynamic terms that is explicitly defined as follows

$$N \triangleq M_f(\dddot{\gamma}_d + \ddot{e}_1 + \dot{e}_2) + \dot{M}_f\left(\ddot{\gamma}_d + \frac{1}{2}r - \ddot{e}_1\right) + e_2 + \dot{B}_f\,. \tag{31}$$

In order to take advantage of the known structure of the uncertainty in the robot dynamics, we can rewrite $N(\cdot)$ as a sum of two auxiliary signals $N_1(t, \gamma, \dot{\gamma}, \ddot{\gamma})$ and $N_2(z)$ as follows

$$N = \underbrace{M_f(\gamma)\,\dddot{\gamma}_d + \dot{M}_f(\gamma,\dot{\gamma})\ddot{\gamma}_d + \dot{B}_f(\gamma,\dot{\gamma},\ddot{\gamma})}_{N_1(\cdot)} + \underbrace{M_f(\gamma)(\ddot{e}_1 + \dot{e}_2) + \dot{M}_f(\gamma,\dot{\gamma})(\frac{1}{2}r - \ddot{e}_1) + e_2}_{N_2(\cdot)} \tag{32}$$

where $z(t) = \left[\begin{array}{ccc} e_1^T(t) & e_2^T(t) & r^T(t) \end{array}\right]^T$ defines a composite error vector. Motivated by the structure of $N_1(\cdot)$, we define a desired variable $N_{1d}(t)$ as follows

$$\begin{aligned} N_{1d}(t) &\triangleq N(\gamma_d, \dot{\gamma}_d, \ddot{\gamma}_d, \dddot{\gamma}_d) \\ &= M_f(\gamma_d)\,\dddot{\gamma}_d + \dot{M}_f(\gamma_d,\dot{\gamma}_d)\ddot{\gamma}_d \\ &\quad + \dot{B}_f(\gamma_d,\dot{\gamma}_d,\ddot{\gamma}_d) \end{aligned} \tag{33}$$

From Property 3 and Remark 4, it is easy to see that $N_{1d}(t), \dot{N}_{1d}(t) \in \mathcal{L}_\infty$. After adding and subtracting $N_{1d}(t)$ to the right-hand side of (30), we have

$$M_f\dot{r} = -\frac{1}{2}\dot{M}_f r - e_2 - \dot{\bar{\tau}}_f + \tilde{N} + N_{1d} \tag{34}$$

where $\tilde{N} \triangleq N - N_{1d}$ is an unmeasurable error signal. After extensive algebraic manipulations (See Appendix A), it can be shown that $\tilde{N}(\cdot)$ can be upper bounded as follows

$$\tilde{N} \leqslant \rho(\|z\|)\,\|z\| \tag{35}$$

where the notation $\|\cdot\|$ denotes the standard Euclidean norm, $\rho(\|z\|) \in \Re$ is a positive non-decreasing function while $z(t) \in \Re^9$ has been previously defined in (32). Based on the structure of (34), (35) as well as the subsequent stability analysis, we propose the following implementable continuous control law to achieve the stated control objectives

$$\begin{aligned} \bar{\tau}_f = &\ (k_s+1)\,e_2(t) - (k_s+1)\,e_2(t_0) \\ &+ \textstyle\int_{t_0}^{t} \left[(k_s+1)\,e_2(\tau) + (\beta_1+\beta_2)\mathrm{sign}(e_2(\tau))\right] d\tau \end{aligned} \tag{36}$$

where k_s, β_1, β_2 are constant positive control gains. After taking the time derivative of (36) and substituting for $\dot{\bar{\tau}}_f(t)$ into (34), we obtain the following closed loop system

$$\begin{aligned} M_f\dot{r} = &\ -\tfrac{1}{2}\dot{M}_f r - e_2 - (k_s+1)r \\ &-(\beta_1+\beta_2)\mathrm{sign}(e_2) + \tilde{N} + N_{1d}. \end{aligned} \tag{37}$$

6 Stability Analysis

Before presenting the main result of this section, we state the following two lemmas which will be invoked later.

Lemma 1 *Let the auxiliary function $L_1(t) \in \Re$ be defined as follows*

$$L_1 \triangleq r^T\left(N_{1d} - \beta_1 sign(e_2)\right). \tag{38}$$

If the control gain β_1 is selected to satisfy the sufficient condition

$$\beta_1 > \|N_{1d}(t)\| + \|\dot{N}_{1d}(t)\|, \tag{39}$$

then

$$\int_{t_0}^{t} L_1(\tau)d\tau \leqslant \zeta_{b1} \tag{40}$$

where the positive constant $\zeta_{b1} \in \Re$ is defined as

$$\zeta_{b1} \triangleq \beta_1\|e_2(t_0)\|_1 - e_2^T(t_0)N_{1d}(t_0). \tag{41}$$

where the notation $\|\cdot\|_1$ denotes the $\mathcal{L}_1$ norm.

Proof: The proof is presented in Appendix B. ∎

Lemma 2 *Let the auxiliary function $L_2(t) \in \Re$ be defined as follows*

$$L_2 \triangleq \dot{e}_2^T\left(-\beta_2 sign(e_2)\right). \tag{42}$$

It is then easy to show that

$$\begin{aligned} \textstyle\int_{t_0}^{t} L_2(\tau)d\tau &= \textstyle\int_{t_0}^{t} \dot{e}_2^T\left(-\beta_2 sign(e_2)\right)d\tau \\ &= \beta_2\|e_2(t_0)\|_1 - \beta_2\|e_2(t)\|_1 \\ &\leqslant \beta_2\|e_2(t_0)\|_1 \triangleq \zeta_{b2} \end{aligned} \tag{43}$$

We now state the main stability result for the proposed controller in the following Theorem.

Theorem 3 *The control law of (36) ensures that all system signals are bounded under closed-loop operation and the tracking error is asymptotically stable in the sense that*

$$\lim_{t\to\infty} e_i^{(j)}(t) = 0 \quad \forall\ i = 1, 2;\ j = 0, 1. \tag{44}$$

Proof: The proof is presented in Appendix C. ∎

We now turn our attention to proving the passivity of the robot manipulator. Integrating both sides of the bottom expression of (82), we obtain

$$\int_{t_0}^{t} \|e_2(\tau)\|_1\, d\tau \leqslant \frac{V(t_0)}{\beta_2} \Rightarrow e_2(t) \in \mathcal{L}_1.$$

Since $e_1(t)$ is related to $e_2(t)$ through a transfer function that is strictly proper and stable, one can use Lemma A.8 of [15] to conclude that $e_1(t) \in \mathcal{L}_1$. Now, utilizing (24), we can also state that $\dot{e}_1(t) \in \mathcal{L}_1$. Next, we define the velocity tracking error

$$e_v = v_d - v \tag{45}$$

where $v_d(t)$ has been previously defined in (6) and $v(t) \in \Re^3$ denotes actual end-effector velocity coordinates in $\mathcal{F}$ such that

$$v = \dot{\gamma} - \dot{s}[u]_\times \gamma. \tag{46}$$

The work done by the interaction force on the robot is denoted by $W(t)$ and given by

$$W = \int_{t_0}^{t} v^T F_f d\tau = \int_{t_0}^{t} v_d^T F_f d\tau - \int_{t_0}^{t} e_v^T F_f d\tau \tag{47}$$

where (45) has been utilized. Since the first term on the right hand side of (47) has been lowerbounded as in (15), we focus our attention on the second term. We expand the second term as follows

$$\int_{t_0}^{t} e_v^T F_f d\tau = \int_{t_0}^{t} \dot{e}_1^T F_f d\tau - \int_{t_0}^{t} \left(\dot{s}[u]_\times e_1\right)^T F_f d\tau$$

where we have utilized (45), (46), (6), and (23). We can now upperbound as follows

$$\begin{array}{rcl} \int_{t_0}^{t} e_v^T F_f d\tau & \leq & \sup_t \{\|F_f(t)\|\} \left[\int_{t_0}^{t} \|\dot{e}_1(t)\|_1 d\tau + \right. \\ & & \left. \sup_t \left\{|\dot{s}(t)| \left\|[u]_\times\right\|\right\} \int_{t_0}^{t} \|e_1(\tau)\|_1 d\tau\right] \\ & \leq & c_2^2 \end{array} \tag{48}$$

where $e_1(t), \dot{e}_1(t) \in \mathcal{L}_1$ has been utilized. Additionally, we have utilized Assumptions 3 and 4 to justify the existence of the supremum functions defined above. One can now utilize the lowerbound of (15) and the upperbound of (48) in order to lowerbound $W(t)$ as follows

$$W(t) \geq -c_1^2 - c_2^2 = -c^2$$

which satisfies the passivity control objective of (26).

7 Unmeasurable Interaction Force Extension

In this Section, we deal with the important problem of compensating for uncertainty or noise in the interaction force measurements at the robot end-effector. Our primary and secondary control objectives remain the same as formulated in Section 4. We work under Assumptions 3-6 made earlier; however, we modify Assumptions 1 and 2 as follows

Assumption 1 The transformed inertia, centripetal-Coriolis, and gravity matrices denoted, respectively, by $M_f(\cdot), C_f(\cdot)$, and $G_f(\cdot)$ are known.

Assumption 2 $F_f(t) \in \mathcal{L}_\infty$ is an unmeasurable interaction force at the end-effector that is second order differentiable.

Since $F_f(t)$ is unmeasurable, we modify the desired end-effector velocity generator as follows

$$M_\Gamma \dot{v}_d + B_\Gamma v_d + k_\Gamma \tilde{\gamma}_d = \hat{F}_f \tag{49}$$

where $\hat{F}_f(t)$ is a yet to be designed interaction force observer while $M_\Gamma, B_\Gamma, k_\Gamma$ have previously been defined in (8). We can now utilize the dynamics of (21) to write an expression for the open loop tracking error dynamics as follows

$$M_f \dot{e}_2 = M_f \ddot{\gamma}_d + M_f \dot{e}_1 + V_f(\gamma, \dot{\gamma})\dot{\gamma} + G_f(\gamma) - \tau_f - F_f \tag{50}$$

where we have utilized the definitions of (23) and (24). Based on Assumptions 1 and 2 as well as the structure of the open-loop dynamics above, we design the control input $\tau_f(t)$ as follows

$$\tau_f = M_f \ddot{\gamma}_d + M_f \dot{e}_1 + V_f(\gamma, \dot{\gamma})\dot{\gamma} + G_f(\gamma) - \hat{F}_f + \tau_{f1} \tag{51}$$

where $\tau_{f1}(t) \in \Re^3$ is an auxiliary control signal that is yet to be defined. After substituting (51) into (50), we can obtain the following expression

$$M_f \dot{e}_2 = -\left(F_f - \hat{F}_f\right) - \tau_{f1} \tag{52}$$

In order to simplify the development of the error system, we define a measurable auxiliary error variable $y(t) \triangleq M_f e_2$. After taking the time derivative of $y(t)$ along the dynamics of (52), we obtain

$$\dot{y} = \dot{M}_f e_2 - \left(F_f - \hat{F}_f\right) - \tau_{f1} \tag{53}$$

We can now design the auxiliary input control input signal as $\tau_{f1}(t) = \dot{M}_f(t) e_2(t)$ in order to obtain the tracking error system as follows

$$\dot{y} = -\left(F_f - \hat{F}_f\right) \tag{54}$$

After introducing a filtered tracking error variable $\bar{r}(t) \triangleq \dot{y} + \bar{\alpha} y$ ($\bar{\alpha}$ a scalar gain constant) and taking its time derivative along the dynamics of 54, we obtain

$$\dot{\bar{r}} = -\left(\dot{F}_f - \dot{\hat{F}}_f\right) + \bar{\alpha}\dot{y} \tag{55}$$

where we have taken advantage of the differentiability of the interaction force. Motivated by our desire to design a continuous controller, we can design the interaction force observation strategy as follows

$$\dot{\hat{F}} = -\bar{k}_s \bar{r} - \bar{\alpha}\dot{y} - (\beta_3 + \beta_4)\,\mathrm{sign}(y) \tag{56}$$

where $\beta_3, \beta_4, \bar{k}_s > 0$ are constant control gains. Since $\bar{r}(t), \dot{y}(t)$ are unmeasurable, an implementable form for (56) is obtained as follows

$$\begin{aligned} \hat{F} &= \left(\bar{k}_s + \bar{\alpha}\right) y(t_0) - \left(\bar{k}_s + \bar{\alpha}\right) y(t) \\ &\quad - \int_{t_0}^{t} \left[(\beta_3 + \beta_4)\,\mathrm{sign}(y(\tau)) + \bar{k}_s \bar{\alpha} y(\tau)\right] d\tau \end{aligned} \tag{57}$$

After substituting (56) into (55), we can obtain the following form for the closed-loop dynamics

$$\dot{\bar{r}} = -\dot{F}_f - \bar{k}_s \bar{r} - (\beta_3 + \beta_4)\,\mathrm{sign}(y) \tag{58}$$

Before we delve into the stability analysis, we state and prove the following lemmas.

Lemma 4 *Let the auxiliary function $L_3(t) \in \Re$ be defined as follows*

$$L_3 \triangleq -\bar{r}^T \left(\dot{F}_f + \beta_3 sgn(y)\right). \tag{59}$$

If the control gain β_3 is selected to satisfy the following sufficient condition

$$\beta_3 > \left\|\dot{F}_f\right\| + \bar{\alpha}^{-1} \left\|\ddot{F}_f\right\|, \tag{60}$$

then

$$\int_{t_0}^{t} L_3(\tau) d\tau \leqslant \zeta_{b3} \tag{61}$$

where the positive constant $\zeta_{b3} \in \Re$ is defined as

$$\zeta_{b3} \triangleq \beta_3 ||y(t_0)||_1 - y^T(t_0) \dot{F}_f(t_0). \tag{62}$$

Proof: *The proof is similar as in Appendix B and obtained by replacing $N_{1d}(t)$ with $-\dot{F}_f(t)$.* ■

Lemma 5 *Let the auxiliary function $L_4(t) \in \Re$ be defined as follows*

$$L_4 \triangleq -\beta_4 \dot{y}^T sgn(y). \tag{63}$$

It is then easy to show that

$$\begin{aligned} \int_{t_0}^{t} L_4(\tau) d\tau &= \int_{t_0}^{t} \left(-\beta_4 \dot{y}^T sgn(y)\right) d\tau \\ &= \beta_4 ||y(t_0)||_1 - \beta_4 ||y(t)||_1 \\ &\leqslant \beta_4 ||y(t_0)||_1 \triangleq \zeta_{b4} \end{aligned} \tag{64}$$

We are now in a position to state the following theorem.

Theorem 6 *The observation and control strategy given by (51) and (57) ensure the boundedness of all system signals and global asymptotic tracking in the sense that*

$$\lim_{t \to \infty} e_i(t), \dot{e}_i(t) = 0 \quad \forall\ i = 1, 2 \tag{65}$$

Proof: The proof is presented in Appendix E. ■

8 Simulation Results

Numerical simulations were performed to illustrate the performance of the proposed reference generator and control law of (6), (8), (10), and (36) with a two-link planar elbow arm whose inertia matrix $M(q)$can be expressed in terms of its elements as follows

$$\begin{aligned} m_{11} &= (m_1 + m_2) l_1^2 + m_2 l_2^2 + 2 m_2 l_1 l_2 \cos q_2 \\ m_{12} &= m_{21} = m_2 l_2^2 + m_2 l_1 l_2 \cos q_2 \\ m_{22} &= m_2 l_2^2 \end{aligned}, \tag{66}$$

while the centripetal Coriolis vector can be expressed in the following manner

$$V_m(q, \dot{q})\dot{q} = \begin{bmatrix} -m_2 l_1 l_2 \left(2\dot{q}_1 \dot{q}_2 + \dot{q}_2^2\right) \sin q_2 \\ m_2 l_1 l_2 \dot{q}_1^2 \sin q_2 \end{bmatrix}. \tag{67}$$

The mass and length parameters of the manipulator are specified as follows

$$\begin{aligned} m_1 &= 8.339 \text{ [kg]} & m_2 &= 0.772 \text{ [kg]} \\ l_1 &= 0.6 \text{ [m]} & l_2 &= 0.5 \text{ [m]} \end{aligned}$$

The initial configuration of the two-link robot are chosen as

$$q_1(0) = 0.2 \text{ [rad]} \qquad q_2(0) = 0.1 \text{ [rad]}$$

The desired contour is specified by a unit circular path $\bar{r}_d(s) = \cos(s)\,\hat{\imath} + \sin(s)\,\hat{\jmath}$. The initial conditions and parameters for the reference generator are chosen as follows

$$\begin{aligned} &\gamma_d(0) = \begin{bmatrix} 0 & -1 \end{bmatrix}^T \text{ [m]} && s(0) = 0 \\ &M_\Gamma = diag\{1, 100\} \text{ [kg]} && B_\Gamma = diag\{4, 1e5\} \text{ [Ns}^{-1}\text{]} \end{aligned}.$$

The interaction force applied at the end-effector was chosen to be $F_f^T = \begin{bmatrix} 2 & 2 \end{bmatrix}$ [N]. For best transient performance, the control gains specified in (36) were chosen to be $k_s = 100, \beta_1 = 0.5, \beta_2 = 0.5$. For different values of stiffness, the following two cases were studied:

Case 1: When the stiffness is selected as $k_\Gamma = 1$ [Nm^{-1}], the circular path can be completed and repeated with the user's applied force. The resulting task-space desired and actual manipulator position as well as the time histories of the position errors are depicted in Figure 1 in Appendix F. Figure 2 in Appendix F shows the joint control inputs $\tau_q(t)$.

Case 2: When stiffness is selected as $k_\Gamma = 2$ [Nm^{-1}], the circular path cannot be completed given the limited amount of applied interaction force. In Appendix F, Figure 3 shows the resulting desired and actual manipulator position and position errors. The control torques $\tau_q(t)$ are depicted in Figure 4 in Appendix F.

References

[1] R. J. Anderson and M.W. Spong, "Bilateral control of teleoperators with time delay", *IEEE Trans. Automat. Contr.*, vol. 34, pp. 494-501, May 1989.

[2] Gregory T. Carter, "Rehabilitation Management in Neuromuscular Disease", *J. Neuro. Rehab.,* 11:69-80, 1997.

[3] J. Engelberger, *Robotics in Service*, Cambridge, Massachussets, The MIT Press, 1989.

[4] B. Hannaford, "A Design Framework for Teleoperators with Kinesthetic Feedback", *IEEE Trans. Robot. Automat.*, vol. 5, pp. 426434, August 1989.

[5] K. Huh, C. Seo, J. Kim, and D. Hong, D "Active SteeringControl Based on the Estimated Tire Forces", *Proceedings of the American Control Conference*, San Diego, CA, pp. 729-733, June 1999.

[6] H. Jeffreys and B. Jeffreys, *Methods of Mathematical Physics*, Cambridge University Press, 3rd edition, Feb. 2000.

[7] P. Kokotovic, "The Joy of Feedback: Nonlinear and Adaptive", *IEEE Control Syst. Mag.*, Vol. 12, pp. 177-185, June 1992.

[8] H.H. Kwee, et al., "The MANUS Wheelchair-Borne Manipulator: System Review and First Results", *Proc. IARP Workshop on Domestic and Medical & Healthcare Robotics*, Newcastle, 1989.

[9] D. A. Lawrence, "Stability and transparency in bilateral teleoperation", *IEEE Trans. Robot. Automat.*, vol. 9, pp. 624-637, Oct. 1993.

[10] D. Lee and P.Y. Li, "Passive Bilateral Feedforward Control of Linear Dynamically Similar Teleoperated Manipulators", *IEEE Trans. Robot. Automat.*, vol. 19, no. 3., pp. 443-456, June 2003.

[11] P.Y. Li and R. Horowitz, "Control of Smart Exercise Machines - Part I: Problem Formulation and Nonadaptive Control", *IEEE Trans. Mechatronics,* vol. 2, no. 4, pp. 237-247, December 1997.

[12] P.Y. Li and R. Horowitz, "Control of Smart Exercise Machines - Part II: Self Optimizing Control", *IEEE Trans. Mechatronics,* vol. 2, no. 4, pp. 247-248, December 1997.

[13] M.Van der Loos, S.Michalowski, and L.Leifer, "Design of an Omnidirectional Mobile Robot as a Manipulation Aid for the Severely Disabled", *Interactive Robotic Aids*, World Rehabilitation Fund Monograph #37 (R. Foulds ed.), New York, 1986.

[14] R.M. Mahoney, "The Raptor Wheelchair Robot System", *Integration of Assistive Technology in the Information Age* (M. Mokhtari, ed.), IOS, Netherlands, pp.135-141, 2001.

[15] M.S. de Queiroz, D.M. Dawson, S. Nagarkatti, F. Zhang, *Lyapunov-Based Control of Mechanical Systems*, Cambridge: Birkhäuser, 2000.

[16] P. Setlur, D.M. Dawson, J. Wagner, and Y. Fang, "Nonlinear tracking Controller Design for Steer-by-wire systems", *Proceedings of the American Control Conference*, Anchorage, AK, pp. 280-285, May 2002.

[17] P. Setlur, D. Dawson, J. Chen, and J. Wagner, "A Nonlinear Tracking Controller for a Haptic Interface Steer-by-Wire Systems", *Proc. of the IEEE Conference on Decision and Control*, Las Vegas, NV, pp. 3112-3117, December 2002.

[18] J.J. Slotine and W. Li, A*pplied Nonlinear Control,* New York: Prentice Hall, 1991.

[19] M. W. Spong and M. Vidyasagar, *Robot Dynamics and Control*, New York: John Wiley and Sons, Inc., 1989.

[20] J.T. Wen, D. Popa, G. Montemayor, P.L. Liu, "Human Assisted Impedance Control of Overhead Cranes," *2001 Conference on Control Applications*, Mexico City, Mexico, Sept. 2001.

[21] B. Xian, M.S. de Queiroz, and D.M. Dawson, "A Continuous Control Mechanism for Uncertain Nonlinear Systems", *Optimal Control, Stabilization, and Nonsmooth Analysis, Lecture Notes in Control and Information Sciences,* Heidelberg, Germany: Springer-Verlag, to appear, 2004.

[22] Y. Yokokohji and T. Yoshikawa, "Bilateral Control of Master-Slave Manipulators for Ideal Kinesthetic Coupling - Formulation and Experiment, *IEEE Trans. Robot. Automat.*, vol. 10, pp. 605-620, Oct. 1994.

8.1 Appendix A. Proof of Bound on $\tilde{N}$

We start by writing $\tilde{N}(t)$ from (31) and (33) as follows

$$\begin{aligned}\tilde{N} = \; & \left[M_f(\gamma) - M_f(\gamma_d)\right] \dddot{\gamma}_d \\ & + \left[\dot{M}_f\left(\gamma,\dot{\gamma}\right) - \dot{M}_f\left(\gamma_d,\dot{\gamma}_d\right)\right] \ddot{\gamma}_d \\ & + \left[\dot{B}_f\left(\gamma,\dot{\gamma},\ddot{\gamma}\right) - \dot{B}_f\left(\gamma_d,\dot{\gamma}_d,\ddot{\gamma}_d\right)\right] \\ & + M_f(\gamma)(\ddot{e}_1 + \dot{e}_2) \\ & + \dot{M}_f\left(\gamma,\dot{\gamma}\right)(\frac{1}{2}r - \ddot{e}_1) + e_2.\end{aligned} \tag{68}$$

To simplify the notation, we define the following auxiliary functions

$$\begin{aligned}\Phi_{bf}(\gamma,\dot{\gamma},\ddot{\gamma}) &\triangleq \dot{B}_f(\gamma,\dot{\gamma},\ddot{\gamma}) \\ \Phi_{mf}(\gamma,\dot{\gamma},\ddot{\gamma}_d) &\triangleq \dot{M}_f(\gamma,\dot{\gamma})\ddot{\gamma}_d\end{aligned} \tag{69}$$

$$E = M_f(\cdot)\ddot{e}_1 + M_f(\cdot)\dot{e}_2 + e_2 + \dot{M}_f(\cdot)\frac{1}{2}r - \dot{M}_f(\cdot)\ddot{e}_1 \tag{70}$$

From (23-25), it is possible to write

$$\dot{e}_1 = e_2 - e_1 \qquad \dot{e}_2 = r - e_2 \qquad \ddot{e}_1 = r - 2e_2 + e_1$$

Given the definitions of (69) and (70), we can rewrite (68) by adding and subtracting a bevy of terms as follows

$$\begin{aligned}\tilde{N} = \; & \left[\bar{M}_f(\gamma) - \bar{M}_f(\gamma_d)\right] \dddot{\gamma}_d \\ & + \left[\Phi_{mf}(\gamma,\dot{\gamma},\ddot{\gamma}_d) - \Phi_{mf}(\gamma_d,\dot{\gamma},\ddot{\gamma}_d)\right] \\ & + \left[\Phi_{mf}(\gamma_d,\dot{\gamma},\ddot{\gamma}_d) - \Phi_{mf}(\gamma_d,\dot{\gamma}_d,\ddot{\gamma}_d)\right] \\ & + \left[\Phi_{bf}(\gamma,\dot{\gamma},\ddot{\gamma}) - \Phi_{bf}(\gamma_d,\dot{\gamma},\ddot{\gamma})\right] \\ & + \left[\Phi_{bf}(\gamma_d,\dot{\gamma},\ddot{\gamma}) - \Phi_{bf}(\gamma_d,\dot{\gamma}_d,\ddot{\gamma})\right] \\ & + \left[\Phi_{bf}(\gamma_d,\dot{\gamma}_d,\ddot{\gamma}) - \Phi_{bf}(\gamma_d,\dot{\gamma}_d,\ddot{\gamma}_d)\right] + E.\end{aligned} \tag{71}$$

Given Assumption 1, we can apply the Mean Value Theorem [6] to each bracketed term of (68) as follows

$$\begin{aligned}\tilde{N} = & \left.\frac{\partial M_f(\sigma_1)}{\partial \sigma_1}\right|_{\sigma_1=\varsigma_1} e_1 \dddot{\gamma}_d \\ & + \left.\frac{\partial \Phi_{mf}(\sigma_5,\dot{\gamma},\ddot{\gamma}_d)}{\partial \sigma_2}\right|_{\sigma_2=\varsigma_2} e_1 \\ & + \left.\frac{\partial \Phi_{mf}(\gamma_d,\sigma_3,\ddot{\gamma}_d)}{\partial \sigma_3}\right|_{\sigma_3=\varsigma_3} \dot{e}_1 \\ & + \left.\frac{\partial \Phi_{bf}(\sigma_4,\dot{\gamma},\ddot{\gamma})}{\partial \sigma_4}\right|_{\sigma_4=\varsigma_4} e_1 \\ & + \left.\frac{\partial \Phi_{bf}(\gamma_d,\sigma_5,\ddot{\gamma})}{\partial \sigma_5}\right|_{\sigma_5=\varsigma_5} \dot{e}_1 \\ & + \left.\frac{\partial \Phi_{bf}(\gamma_d,\dot{\gamma}_d,\sigma_6)}{\partial \sigma_6}\right|_{\sigma_6=\varsigma_6} \ddot{e}_1 + E\end{aligned} \tag{72}$$

where $\varsigma_1(t), \varsigma_2(t), \varsigma_4(t) \in (\gamma, \gamma_d)$, $\varsigma_3(t), \varsigma_5(t) \in (\dot{\gamma}, \dot{\gamma}_d)$ while $\varsigma_6(t) \in (\ddot{\gamma}, \ddot{\gamma}_d)$. From the preceding analysis, the right-hand side of (72) can be succinctly expressed as

$$\tilde{N} = \Phi z. \tag{73}$$

where $z(t) \in \mathbb{R}^{9\times 1}$ is the composite error vector that has previously been defined and $\Phi(\gamma, \dot{\gamma}, \ddot{\gamma}, t) \in \mathbb{R}^{3\times 9}$ is the first-order differentiable system regressor. By virtue of its first-order differentiability, $\Phi(\cdot)$ can be upperbounded as follows

$$\Phi(\gamma, \dot{\gamma}, \ddot{\gamma}, t) \leq \bar{\rho}(\gamma, \dot{\gamma}, \ddot{\gamma}) \tag{74}$$

where $\bar{\rho}(\cdot)$ is a positive function nondecreasing in $\gamma(t), \dot{\gamma}(t)$, and $\ddot{\gamma}(t)$. Given Assumption 3, we can utilize (74) and the facts that

$$\begin{aligned}\gamma &= \gamma_d - e_1 \\ \dot{\gamma} &= \dot{\gamma}_d - e_2 + e_1 \\ \ddot{\gamma} &= \ddot{\gamma}_d - r + 2e_2 - e_1\end{aligned}$$

in order to upperbound $\tilde{N}(\cdot)$ as follows

$$\tilde{N} \leqslant \rho(\|z\|)\|z\|$$

where $\rho(\|z\|)$ is some positive function nondecreasing in $\|z\|$.

9 Appendix B: Proof of Lemma 1

After substituting (25) into (38) and then integrating in time, we obtain

$$\begin{aligned}\int_{t_0}^{t} L(\tau)d\tau = & \int_{t_0}^{t} e_2^T(\tau)\left(N_{1d}(\tau) - \beta_1 \text{sgn}(e_2(\tau))\right)d\tau \\ & + \int_{t_0}^{t} \frac{de_2^T(\tau)}{d\tau} N_{1d}(\tau)d\tau \\ & - \beta_1 \int_{t_0}^{t} \frac{de_2^T(\tau)}{d\tau} \text{sgn}(e_2(\tau))d\tau \ .\end{aligned} \tag{75}$$

After integrating the second term on the right-hand side of (75) by parts, we obtain the following simplified expression

$$\begin{aligned}\int_{t_0}^{t} L(\tau)d\tau = & \int_{t_0}^{t} e_2^T(\tau)\Big(N_{1d}(\tau) \\ & - \frac{dN_{1d}(\tau)}{d\tau} - \beta_1 \text{sgn}(e_2(\tau))\Big)d\tau \\ & + e_2^T(t)N_{1d}(t) - e_2^T(t_0)N_{1d}(t_0) \\ & - \beta_1\|e_2(t)\|_1 + \beta_1\|e_2(t_0)\|_1 \ .\end{aligned} \tag{76}$$

We can now upper bound the right-hand side of (76) as follows

$$\begin{aligned}\int_{t_0}^{t} L(\tau)d\tau \leqslant & \int_{t_0}^{t} \|e_2(\tau)\|_1 \left(\|N_{1d}(\tau)\| \right. \\ & \left. + \left\|\frac{dN_{1d}(\tau)}{d\tau}\right\| - \beta_1\right)d\tau \\ & + \|e_2(t)\|_1 \left(\|N_{1d}(t)\| - \beta_1\right) \\ & + \beta_1\|e_2(t_0)\|_1 - e_2^T(t_0)N_{1d}(t_0) \ .\end{aligned} \tag{77}$$

From (77), it is easy to see that if β_1 is chosen according to (39), then (40) holds.

10 Appendix C: Proof of Theorem 3

Let us define two auxiliary functions $P_i(t) \in \Re$ as follows

$$P_i(t) \triangleq \zeta_{bi} - \int_{t_0}^{t} L_i(\tau)d\tau \geqslant 0 \ \forall \ i = 1, 2 \tag{78}$$

where $\zeta_{bi}, L_i(t)$ have been previously defined in Lemmas 1 and 2. Based on the non-negativity of $P_i(t)$ above, one can define a nonnegative function $V(t)$ as follows

$$V \triangleq \frac{1}{2}e_1^T e_1 + \frac{1}{2}e_2^T e_2 + \frac{1}{2}r^T M_f r + P_1 + P_2 \tag{79}$$

After taking the time derivative of (79) and utilizing the definitions of (23-25) as well as the closed-loop dynamics of (37), we can conveniently rearrange the terms to obtain the following expression for $\dot{V}(t)$

$$\begin{aligned}\dot{V} = & -\|e_1\|^2 - \|e_2\|^2 - (k_s+1)\|r\|^2 \\ & + e_1^T e_2 + r^T\tilde{N} - \beta_2 e_2^T sgn(e_2) \\ & + \left[r^T\left(N_{1d} - \beta_1 \text{sign}(e_2)\right) - L_1\right] \\ & - \left[\dot{e}_2^T\beta_2 \text{sign}(e_2) + L_2\right]\end{aligned} \tag{80}$$

where we have utilized the definition of (78). After utilizing the definitions of (38) and (42) to eliminate the bracketed terms in the above equality, we can utilize simple algebraic manipulations to obtain the following upperbound for $\dot{V}(t)$

$$\dot{V} \leq -\frac{1}{2}\|z\|^2 + \left[\|r\|\rho(\|z\|)\|z\| - k_s\|r\|^2\right] - \beta_2\|e_2\|_1$$

where $z(t)$ is a composite error vector that has been defined previously in (32). Applying the nonlinear damping argument [7] to the bracketed term above, we obtain the following upperbound for $\dot{V}(t)$

$$\dot{V} \leqslant -\frac{1}{2}\left(1 - \frac{\rho^2(\|z\|)}{2k_s}\right)\|z\|^2 - \beta_2\|e_2\|_1 \tag{81}$$

From (81), it is possible to state that

$$\left.\begin{aligned}\dot{V} &\leqslant -\alpha\|z\|^2 \\ \dot{V} &\leqslant -\beta_2\|e_2\|_1\end{aligned}\right\} \text{ for } k_s > \frac{1}{2}\rho^2(\|z\|) \tag{82}$$

where $\alpha \in \Re$ is some positive constant of analysis. We note here that it is possible to express the lowerbound

on k_s in terms of the initial conditions of the problem which has been referred to in literature as a semi-global stability result. We refer the interested reader to Appendix D for the details of such a procedure. Here onward, our analysis is valid in the region of attraction denoted by Ω_c in (86). From (82) and the analysis in Appendix C, it is easy to see that $z(t) \in \mathcal{L}_\infty \cap \mathcal{L}_2$ and $\lim_{t\to\infty} \|z\|^2 = 0$. From the previous assertions and the definitions of (24), (25), and (32), one readily obtains the result of (44).

11 Appendix D: Calculation of Region of Attraction

Following [21], we now define the region of attraction for the system. From (82), we obtain the following sufficient condition for the negative definiteness of $\dot{V}(t)$

$$\|z\| < \rho^{-1}(\sqrt{2k_s}) \tag{83}$$

Next, we define $\eta(t) = [\ z^T(t) \quad \sqrt{P_1(t)} \quad \sqrt{P_2(t)}\ ]^T \in \Re^{11}$ and a region Ω in state space as follows

$$\Omega = \left\{ \eta \in \mathbb{R}^{11} \left| \|\eta\| < \rho^{-1}(\sqrt{2k_s}) \right. \right\} \tag{84}$$

where the definition of $\eta(t)$ indicates that Ω is a subset of the space defined by (83). Based on Assumption 3 in Section 4, we define $\delta_1 \triangleq \frac{1}{2}\min\{1, \underline{m}\}$ and $\delta_2(\gamma) \triangleq \max\left\{\frac{1}{2}\overline{m}(\gamma), 1\right\}$; thereby, (79) can be upper and lower bounded as

$$\xi_1(\eta) \leq V \leq \xi_2(\eta) \tag{85}$$

where $\xi_1(\eta) \triangleq \delta_1 \|\eta\|^2 \in \Re$ and $\xi_2(\eta) \triangleq \delta_2(\gamma)\|\eta\|^2 \in \Re$. From the boundedness conditions above, we can further find an estimate for the region of attraction of the system as

$$\Omega_c = \left\{ \eta \in \Omega \left| \xi_2(\eta) < \delta_1(\rho^{-1}(\sqrt{2k_s}))^2 \right. \right\} \tag{86}$$

Given (85) and (82), we can invoke Lemma 2 of [21] to state that

$$\lim_{t\to\infty} \|z\|^2 = 0 \ \forall\ \eta(t_0) \in \Omega_c\ . \tag{87}$$

From (86), we require

$$\xi_2(\eta(t)) < \delta_1(\rho^{-1}(\sqrt{2k_s}))^2 \tag{88}$$

which implies that we can write (88) in terms of system initial conditions as follows

$$\|\eta(t_0)\| < \sqrt{\frac{\delta_1}{\delta_2(\gamma(t_0))}}\rho^{-1}(\sqrt{2k_s}), \tag{89}$$

where we have taken advantage of the fact that $V(t)$ is either decreasing or constant for all time. We can rewrite (89) in terms of an lowerbound on k_s as follows

$$k_s > \frac{1}{2}\rho^2\left(\sqrt{\frac{\delta_2(\gamma(t_0))}{\delta_1}}\,\|\eta(t_0)\|\right). \tag{90}$$

Given the definition of $\eta(t)$, we can write

$$\begin{aligned}\|\eta(t_0)\| = \ & \big(e_1^T(t_0)e_1(t_0) + e_2^T(t_0)e_2(t_0) \\ & + [\dot{e}_2(t_0) + e_2(t_0)]^T[\dot{e}_2(t_0) + e_2(t_0)] \\ & + P_1(t_0) + P_2(t_0)\big)^{\frac{1}{2}}\end{aligned} \tag{91}$$

where we have utilized the definitions of $z(t)$ and $r(t)$ from (32) and (25). From (41), (43), (23), and (29), we can obtain the following expression

$$\begin{aligned}\dot{e}_2(t_0) = \ & \ddot{\gamma}_d(t_0) + \dot{\gamma}_d(t_0) - \dot{\gamma}(t_0) \\ & + M_f^{-1}(\gamma(t_0))B_f(\gamma(t_0), \dot{\gamma}(t_0))\ .\end{aligned}$$

After substituting the above expression into (91), we can finally express $\|\eta(t_0)\|$ in terms of system initial conditions as follows

$$\begin{aligned}\|\eta(t_0)\| = \ & \Big(e_1^T(t_0)e_1(t_0) + e_2^T(t_0)e_2(t_0) \\ & \Big\|\ddot{\gamma}_d(t_0) + M_f^{-1}(\gamma(t_0))B_f(\gamma(t_0), \dot{\gamma}(t_0)) \\ & + \dot{\gamma}_d(t_0) - \dot{\gamma}(t_0) + e_2(t_0)\Big\|^2 \\ & + \beta_1\|e_2(t_0)\|_1 - e_2^T(t_0)N_{1d}(t_0) \\ & + \beta_2\|e_2(t_0)\|_1\Big)^{1/2}\ .\end{aligned} \tag{92}$$

12 Appendix E: Proof of Theorem 6

To prove this theorem, we utilize the following non-negative function

$$V \triangleq \frac{1}{2}\bar{r}^T\bar{r} + P_3 + P_4 \tag{93}$$

where the two auxiliary functions $P_3(t), P_4(t) \in \Re$ are defined as follows

$$P_i(t) \triangleq \zeta_{bi} - \int_{t_0}^{t} L_i(\tau)d\tau \geqslant 0\ \forall\ i = 3, 4 \tag{94}$$

After taking the time derivative of (93) along (58), we can upperbound $\dot{V}(t)$ as follows

$$\dot{V}(t) \leq -k_s\|\bar{r}\|^2 - \bar{\alpha}\beta_4\|y\|_1$$

where we have utilized the definitions of (59), (63), and (94). It is now easy to show that $\bar{r}(t), y(t) \in \mathcal{L}_\infty \cap \mathcal{L}_2$. From the previous assertions and the definitions of (24) and (25), we can now use Lemma A.8 of [15] to state that $e_1(t), \dot{e}_1(t), e_2(t), \dot{e}_2(t) \in \mathcal{L}_1 \cap \mathcal{L}_\infty$. Given these assertions and some signal chasing akin to the proof of Theorem 3, we can obtain the control objectives targeted in Section 4.

13 Appendix F: Simulation Plots

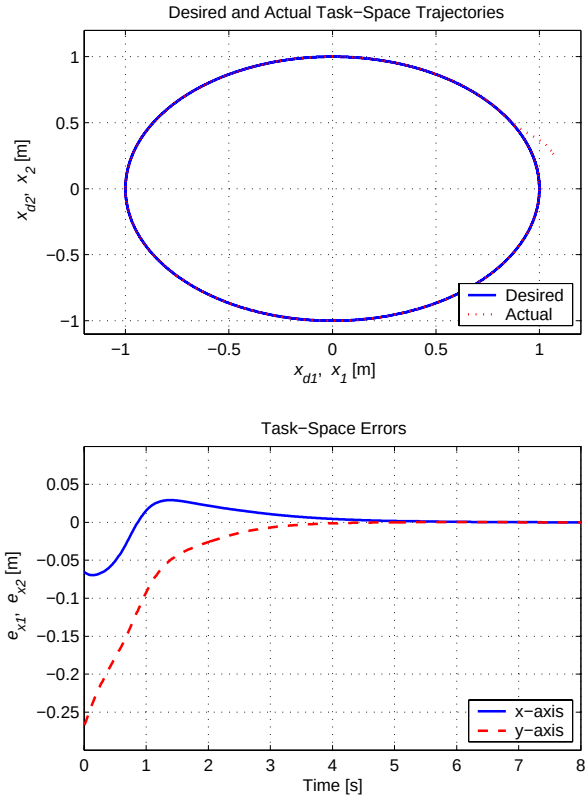

Figure 1: Workspace Trajectories and Errors : $k_\Gamma = 1$

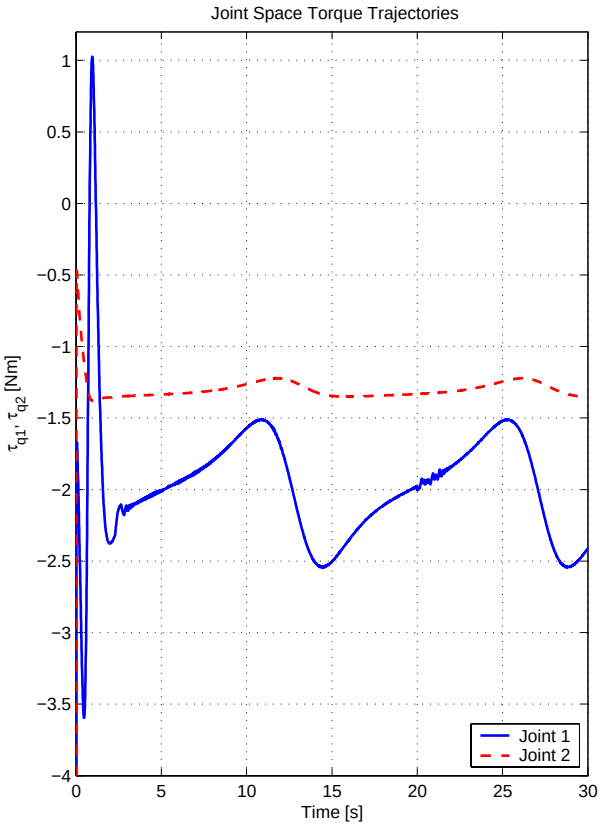

Figure 2: Robot Joint Torque Inputs: $k_\Gamma = 1$

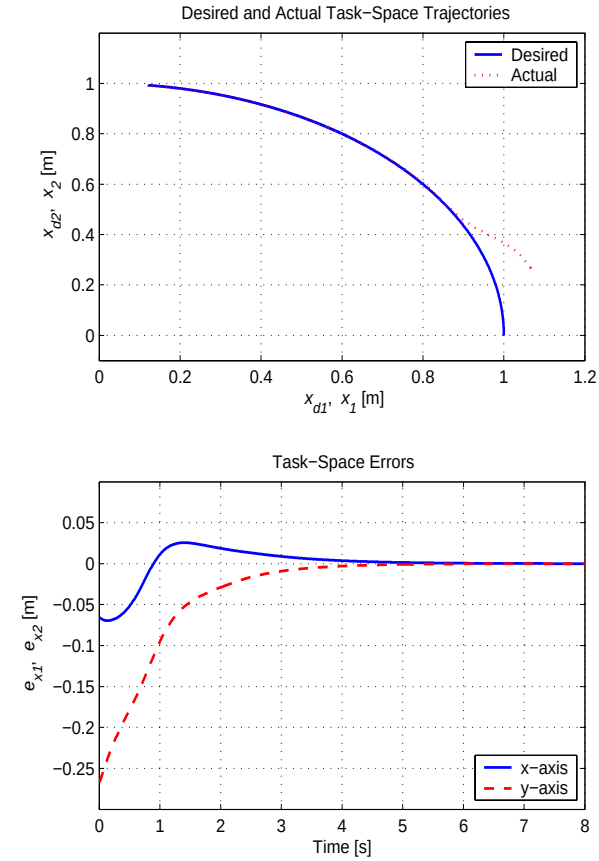

Figure 3: Workspace Trajectories and Errors : $k_\Gamma = 2$

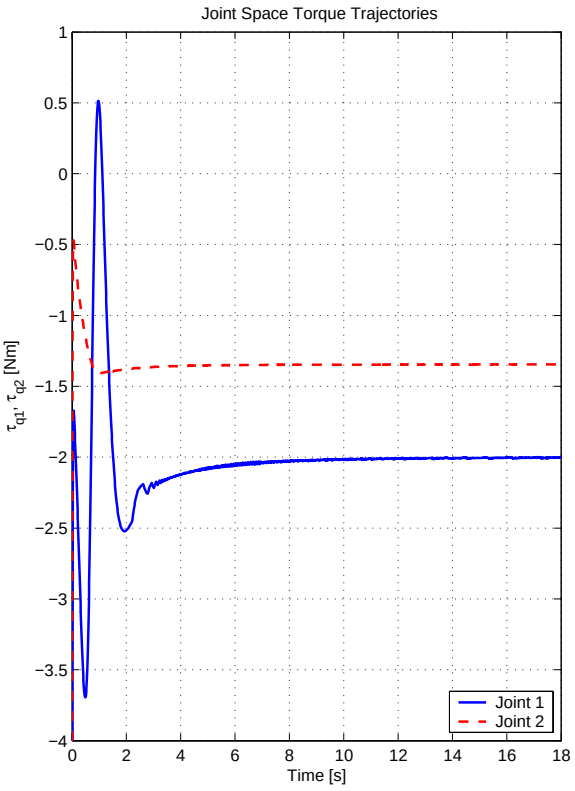

Figure 4: Robot Joint Torque Inputs: $k_\Gamma = 2$